ChemPubSoc Europe

DOI: 10.1002/cbic.201800679

CHEMBIOCHEM Communications

Macromolecular Crowding Tunes Protein Stability by Manipulating Solvent Accessibility

Birgit Köhn[a, b] and Michael Kovermann*[a, b]

In all intracellular processes, protein structure and dynamics are subject to the influence of macromolecular crowding (MC). Here, the impact of MC agents of different types and sizes on the model protein *Bacillus subtilis* Cold shock protein B (*Bs*CspB) during both thermal and chemical denaturation have been comprehensively investigated. We consistently reveal a distinct stabilization of *Bs*CspB in a manner dependent on the MC concentration but not on viscosity, polarity, or size of the MC agent used. This general stabilization has been decoded by use of NMR spectroscopy, through monitoring of chemical shift (CS) perturbations and the intramolecular hydrogen-bonding networks, as well as local protection of amide protons against exchange with solvent protons. Whereas CSs and hydrogen-bonding networks are not systematically affected in the presence of MC, we detected a pronounced reduction in exchange in loop regions of *Bs*CspB. We conclude that this reduced accessibility of solvent protons is a key parameter for the increases in protein stability seen under MC.

In all living organisms, protein folding and function takes place in highly crowded environments, containing up to 400 g L^{-1} of macromolecules in solution.[1] In harsh contrast, most if not all biochemical studies on proteins are conducted in the presence merely of a buffering agent and a few ligands or reactants, thus resulting in a strongly diluted environment. Inherently, these conditions do not mirror the intracellular milieu because the structural, dynamic, and functional properties of proteins are highly dependent on minute changes in conformation and stability. Moreover, the limited access to specific sites of interaction can easily be perturbed by slight changes in the chemical environment. Consequently, biological mechanisms and conformational ensembles that might be encountered in vivo are therefore obviously different from in vitro scenarios.[2] A comprehensive understanding of all processes taking place in vivo is essential not only from a biochemical point of view but even more so from medical perspectives, in view of, for example, the formation of protein aggregates and amyloid structures causing diseases such as amyotrophic lateral sclerosis (ALS), Alzheimer's and Parkinson's disease, or diabetes type 2.

The key to an in-depth understanding of proteostasis is to decode the cellular interior, which is, first of all, a highly crowded place. Recent developments in the field of MC have moved from the viewpoint of a purely entropic excluded volume (EV) effect to a complex interplay of enthalpic "soft" or "chemical interactions" that either contribute to or mitigate the EV effect.[3] Further, the role of charge–charge interactions[4] and protein surfaces has been particularly debated in view of "in-cell" experiments[5] and simulation studies[6] that have transformed perspectives on cells as "bags full of proteins" to cellular "protein droplets".[7] However, in spite of the advances in the field of macromolecular crowding (MC) since 1981,[8] there is to this day no bottom-up concept that allows the direct translation of in vitro data relating to protein structure, dynamics, and function to in vivo scenarios, as Minton, who coined the term "macromolecular crowding" over 30 years ago, just recently pointed out.[9]

Direct in vivo experiments at the resolutions required for the comprehensive study of protein ensembles are seldom possible, and individual contributions of molecular effects cannot be discriminated, so we present here a systematic bottom-up approach based on orthogonal experiments mimicking the crowded intracellular milieu. We decided to use the polymeric crowding agents dextran as well as poly(ethylene glycol) (PEG) of various sizes in order to focus on the influence both of size and of polarity of MC. With regard to hydrophobic side effects of PEG as an inert crowding agent, our model protein—unlike, for example, cytochrome *c*[10a]—is not prone to specific interactions between PEG and hydrophobic surface patches (see below). Similarly, PEG is capable of increasing the stability of RNase A but seems not to interact directly with this protein.[10b] By using synthetic polymers, both steric and electrostatic effects can be observed, whereas further specific interactions that arise when using protein crowders are excluded and the experimental results can be unambiguously assigned to the MC properties that make up the focus of our study. This systematic experimental bottom-up approach is of increased importance due to the fact that numerous contributions in the field of MC are biased by, firstly, the use only of a single type of a crowding agent, secondly, by using a single experimental technique that does not permit comparison with results of alternative methods and, thirdly, by a focus on highly complex systems.[2e,11]

Our study provides a systematic approach applied to the *Bacillus subtilis* Cold shock protein B (*Bs*CspB),[12a,b] which is a

[a] B. Köhn, Prof. Dr. M. Kovermann
Fachbereich Chemie, Universität Konstanz
Universitätsstrasse 10, 78457 Konstanz (Germany)
E-mail: michael.kovermann@uni-konstanz.de

[b] B. Köhn, Prof. Dr. M. Kovermann
Research School Chemical Biology (KoRS-CB), Universität Konstanz
Universitätsstrassee 10, 78457 Konstanz (Germany)

Supporting information and the ORCID identification numbers for the authors of this article can be found under https://doi.org/10.1002/cbic.201800679.

prominent example of a two-state system from the point of view of the folding to unfolding transition.[12c] We have comprehensively investigated and analyzed the impact of MC as induced by crowding agents of different types and sizes present in a broad range of concentrations, with monitoring through a variety of techniques. This has enabled us, in a convergent manner, to understand the thermodynamic origin of the MC effect generally.

Starting with chemical denaturation through the presence of urea, we found a strong stabilization of the native state of *Bs*CspB upon addition of PEG8 as monitored by fluorescence spectroscopy (Figure 1 A, Table S1 in the Supporting Information). At 20% (*w/v*) PEG8 in solution, the stabilization of *Bs*CspB is so remarkable that the fully denatured state cannot be reached in the range of solubility of urea and PEG8 (Figure S1). Interestingly, the addition of PEG1 stabilized *Bs*CspB to the same extent as did PEG8, which is an MC agent of similar molecular weight to the model protein used (Figure 1 B, Table S1). This increase in stability equals the effect of PEG8, thus showing that stabilization of *Bs*CspB is independent of the given viscosity, which differs by a factor of five on comparison of PEG1 with PEG8 for 20% (*w/v*) (Table S2).

Next, we used guanidinium chloride (GdmCl), a stronger and more polar denaturant, to unfold *Bs*CspB chemically. Both with PEG8 and with PEG1 we found stabilization of *Bs*CspB to the same extent as seen with urea (Figure 1 C, D, Table S1). Surprisingly, on comparing PEG with the polar MC agent Dex20, we came to a straightforward result: the increase in the transition midpoint (c_M) is of the same extent on comparing 10% (*w/v*) PEG8 with 10% (*w/v*) Dex20 in the cases both of urea- and of GdmCl-induced denaturing (Figure 1 E, F, Table S1).

So far we can summarize that the stabilizing effect of MC agents on chemical unfolding of *Bs*CspB is only dependent on the volume fraction of the crowder in solution and neither on the size or the polarity of the crowding agent, nor on the charge of the denaturant, nor on the viscosity of the buffer. Mechanistically, this can be interpreted as a pure excluded volume effect, because the volume occupied by the crowding agent is the only shared factor that governs the increase in stability towards chemical unfolding. In other words, *Bs*CspB acts as an ideal system in which both the less polar PEG and the polar Dex macromolecules can equally be considered inert crowding agents.

In a next step, thermal denaturation of *Bs*CspB in the presence of MC was applied to evaluate whether the stabilization seen so far is only dependent on chemical unfolding or if it can be thermodynamically generalized by confirmation in an experimentally different setup. It should be noted that, in contrast with chemical unfolding, the analysis of thermal unfolding by use only of a single parameter is not possible. The change in thermodynamic stability is reflected neither solely in the temperature midpoint (T_m), nor exclusively in the change in enthalpy (ΔH), nor uniquely in the difference in the heat capacity (ΔC_p), but might result from changes in any one, two, or all of these three parameters (see discussion in the Supporting Information). Thermal unfolding transitions for *Bs*CspB as monitored by circular dichroism (CD) spectroscopy in the absence and in the presence of 10, 20, and 30% (*w/v*) PEG8 (Figure 2 A, Table S3) or Dex20 (Figure 2 B, Table S3) show a pronounced increase in T_m in the case of Dex20 but only an extenuated one in that of PEG8. In contrast, ΔH shows a strong increase with rising PEG8 concentration whereas increasing Dex20 concentration does not affect ΔH significantly (Figure 2 C, Table S3). These divergent effects of MC agents seen for the thermal denaturation of *Bs*CspB have also been noted previously in the cases of, for example, ubiquitin[13] and lysozyme.[14]

We additionally monitored the thermal denaturation of partially denatured samples of *Bs*CspB by using 1, 2, or 3 M urea in

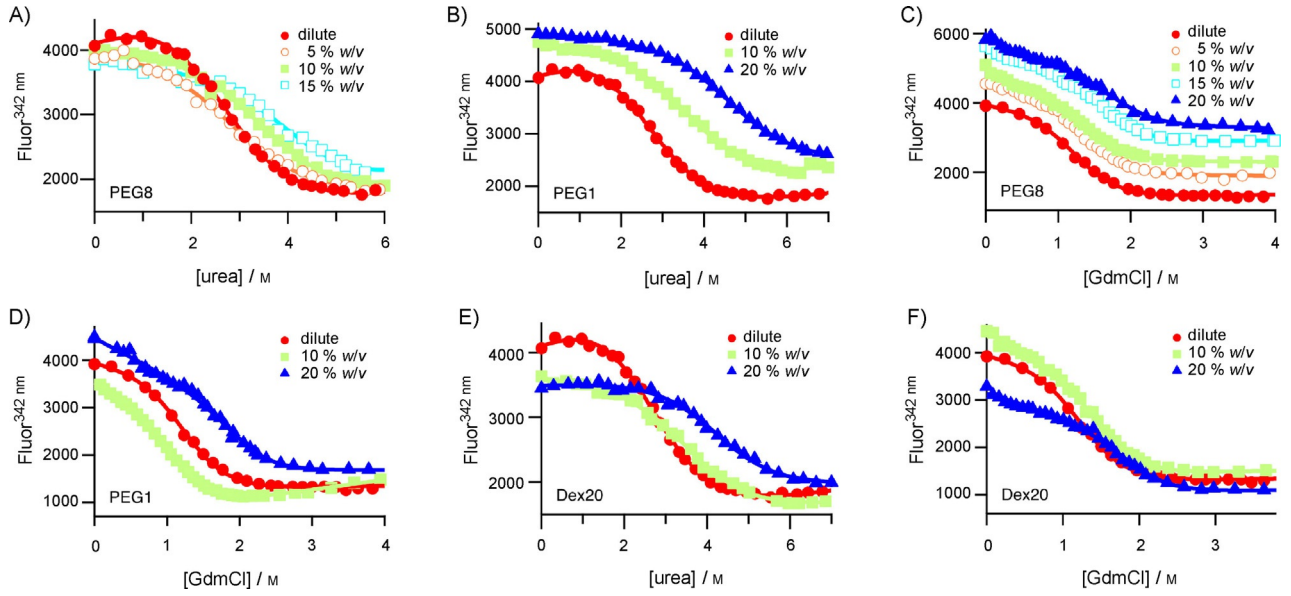

Figure 1. Chemical unfolding of *Bs*CspB, as monitored by fluorescence spectroscopy, induced by increasing amounts of A), B), E) urea, or C), D), F) GdmCl and in the presence of varying concentrations of the MC agents A), C) PEG8, B), D) PEG1, or E), F) Dex20. Experimental data are shown as symbols whereas global data fitting to a two-state folding model are represented by straight lines. Fitting values for the overall stability (ΔG) and the cooperativity of folding (m) are given in Table S1.

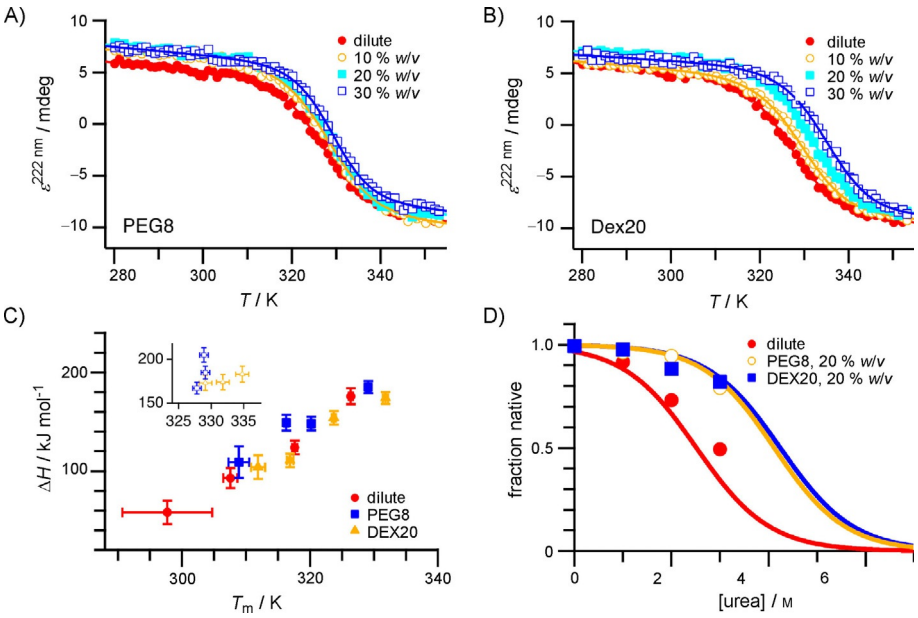

Figure 2. Thermally induced unfolding of *Bs*CspB as monitored by CD spectroscopy in the presence of dilute (●), 10 (○), 20 (■), or 30% (*w/v*) (□) A) PEG8, or B) Dex20. Experimental data are shown as symbols whereas data fitting to a two-state folding model are represented by straight lines. Fitting values for the change in enthalpy (ΔH) and the midpoint of the transition (T_m) are given in Table S3. C) The values of ΔH and T_m depend on the amount of urea added to *Bs*CspB present at dilute, 20% (*w/v*) PEG8, or 20% (*w/v*) Dex20 conditions (Figure S2 and Table S3). The inset refers to the fitted data obtained in (A) (■) and (B) (▲). D) The overall stability of *Bs*CspB as determined by fluorescence (lines) agrees very well with data obtained by using circular dichroism spectroscopy (symbols).

combination with 0 or 20% (*w/v*) PEG8 or 20% (*w/v*) Dex20, thus being able to contrast the changes in free energy (ΔG) as observed for chemically induced unfolding with those in the thermally induced case (Figures 2C, D and S2, Table S3). Remarkably, this analysis illuminates a general stabilization effect of *Bs*CspB due to addition of MC agents regardless of chemical or thermal unfolding or rather of the technique employed. So far we can conclude that, regardless of the size and polarity of the MC agent added to the solution, solely the weight volume fraction determines the increase in ΔG value of *Bs*CspB (Figure 2D).

What molecular mechanism causes this stabilization? We turned to high-resolution NMR spectroscopy to unravel potential local sites in *Bs*CspB causing the overall stabilization seen by both fluorescence and CD spectroscopy. Firstly, thermal denaturation of *Bs*CspB (Figure S3A) as probed by one-dimensional proton NMR spectroscopy in the presence of various amounts of PEG1 or PEG35 yielded results similar to those seen with PEG8 (Figure S3B–D, Table S4), thus confirming the analysis performed with CD spectroscopy. This agreement was further verified by using Dex20 as MC agent for thermal denaturation of *Bs*CspB (Figure S3E, Table S4). Moving on, the stepwise addition of PEG1, PEG8, PEG35, or Dex20 to ^{15}N-labeled *Bs*CspB (Figure S4A) induced moderate chemical shift perturbations (CSPs) in two-dimensional ^{1}H,^{15}N HSQC spectra (Figure S4B–E). It is notable that neither the amplitudes nor the sequence-dependent courses of these changes match when PEG is compared with Dex20 (Figure S4F–I). Moreover, comparison between residues experiencing CSPs significant larger than the mean as induced by PEG8 or Dex20 does not provide a general pattern even if the inherent properties of single amino acid residues are taken into account (Figure S4J–M). We conclude that the structural characteristics of native *Bs*CspB are highly conserved even when PEG or Dex20 is present.

What contributions, then, lead to the gain in stability seen for the native state of *Bs*CspB if MC is present? We examined the hydrogen-bonding > network by assessment of temperature coefficients (TCs),[15] finding a small number of subtle changes in the general pattern of the network (Figure S5A–D). Note that the local hydrogen-bonding network present in *Bs*CspB is nicely reproduced by using this method (Figure S5E, F). Again, however, detailed analysis of the TCs' dependence on amounts of MC agent added also does not give a general explanation for the monotonic increase in ΔG as presented in Figures 1 and 2D.

Additionally, we determined the exchange of the amide protons (NHs) with solvent water protons by NMR spectroscopy with use of a modified Mexico[16] sequence to characterize the dynamic features of the NHs contained in *Bs*CspB on a millisecond timescale (Figure S6A–F). On comparing the exchange rate constants (k_{ex}) in dilute solution with those in crowded solution we observed three effects (Figure 3A–C). Firstly, an increasing concentration of MC agents equalizes the mean of all k_{ex} values observed in the following manner: $k_{ex}^{dilute} = (3.2 \pm 8.5)\ s^{-1}$, $k_{ex}^{PEG8k} = (2.5 \pm 4.8)\ s^{-1}$, $k_{ex}^{Dex20,\ 12wv} = (1.8 \pm 4.1)\ s^{-1}$, and $k_{ex}^{Dex20,\ 24wv} = (1.5 \pm 2.4)\ s^{-1}$. Secondly, a decrease in the mean of k_{ex} values in the presence of increasing concentrations of MC agents is seen. Thirdly, a pronounced decrease in k_{ex} values of residues present in less protected loop regions and a parallel soft increase in k_{ex} values of residues present in β-sheet positions, which were well protected in dilute conditions (Figure 3A), is apparent. This holds for Dex20 more than for PEG8,

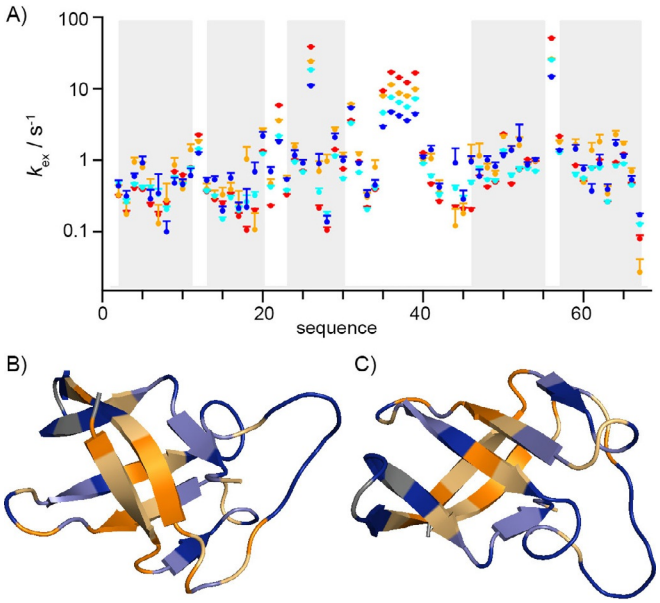

Figure 3. A) The accessibility of the amide protons in *Bs*CspB depends on the amounts of MC agent added. The exchange rate constants (k_{ex}) were determined in the absence (●) and in the presence of 15% (*w/v*) PEG8 (●), 12% (*w/v*) Dex20 (●), or 24% (*w/v*) Dex20 (●) by use of a modified Mexico sequence (cf. Figure S6). Residues comprising β-sheets are indicated by use of a background colored in light gray. B), C) *Bs*CspB (PDB ID: 1NMG) has been colored according to decreases (blue) or increases (orange) in exchange rate constants upon addition of 12% (*w/v*) Dex20, relative to dilute conditions. Dark blue: $\Delta k_{ex} < -0.1$ s^{-1}. Light blue: $-0.1 < \Delta k_{ex} < 0$ s^{-1}. Light orange: $0 < \Delta k_{ex} < 0.1$ s^{-1}. Dark orange: $\Delta k_{ex} > 0.1$ s^{-1}. Gray: n.a.

independently of the increase in viscosity (Table S2) but increasing with volume percentage of crowder in solution.

Two key conclusions can be derived from this. First of all, crowder polarity might play a crucial role in defining the protection effect against exchange of NHs with solvent protons. Thus, the more polar crowder Dex induced stronger protection than the less polar PEG8, which points to the important difference in electrostatic interactions offered by these two different MC agents. This correlates well with the difference between PEG and Dex20 seen in thermal (Figures 2, S2, and S3, Tables S3 and S4) but not in chemical unfolding (Figure 1, Table S1). Most likely, in chemical unfolding this difference in electrostatics between the polyether PEG and the polyalcohol Dex is covered by the presence of the strongly polar co-solute urea and even more so by increasing ionic strength in the presence of GdmCl.[17]

Secondly, the increase in protection as observed increases monotonously with crowder concentration. Because very mobile NHs are readily prone to exchange with water protons, due to the absence of a hydrogen bond (Figure S6G, H), the increased protection of those flexible and highly mobile regions points to a decrease in mobility. In other words, more rigid loop regions contribute to increased thermodynamic stability of the native state of *Bs*CspB if MC is present. This increase in loop rigidity contributing to the native state stability is more pronounced in the case of Dex than in that of PEG, presumably due to electrostatic interactions. Notably, both MC agents are able to induce qualitatively a similar trend towards stabilization. The β-sheet regions of *Bs*CspB show only small changes in exchange rate constants of NHs upon addition of MC agents.

In this study we have applied a systematic approach to understand the impact of MC on the stability of a native protein at atomic resolution in a convergent manner. We have precisely investigated the chemically and thermally induced unfolding of *Bs*CspB by use of fluorescence, CD, and NMR spectroscopic experiments under a multiplicity of different MC conditions. A comprehensive thermodynamic analysis of the acquired data has allowed us to come to a systematic conclusion on the MC effect on *Bs*CspB: we find it to depend solely on the weight per volume fraction added, and not on the type of macromolecule used to mimic MC nor on its size. We can thus show that the thermodynamic stability of *Bs*CspB can be specifically adjusted through addition of a macromolecular compound, regardless of its properties, merely and simply through the macromolecular presence at concentrations similar to those in vivo. High-resolution NMR spectroscopy has illuminated the fact that MC agents significantly reduce the exchange of mobile NHs that are not involved in hydrogen bonding with solvent protons—again, independently of the type of MC agent but in a manner dependent on the weight per volume fraction added. We conclude that this increase in rigidity acts as a driving force for the thermodynamic stabilization of *Bs*CspB if MC is present. This stabilization arises from a modified accessibility of NHs to the solvent, thus resulting in a different microenvironment in that presence of MC from that in the dilute scenario. We speculate that this change in solvent accessibility unraveled here in the case of *Bs*CspB holds as a general explanation for the MC effect affecting the thermodynamic stability of proteins.

Acknowledgements

We thank Iljas Müller and Julian Schuck for support in the initial stage of this project and Hauke Paulsen for graphical assistance. Financial support from the Young Scholar Fund of the Universität Konstanz and from the Collaborative Research Centre 969 funded by the German Research Foundation is gratefully acknowledged.

Conflict of Interest

The authors declare no conflict of interest.

Keywords: biophysics · molecular crowding · NMR spectroscopy · protein folding · thermodynamics

[1] a) S. Cayley, B. A. Lewis, H. J. Guttman, M. T. Record, *J. Mol. Biol.* **1991**, *222*, 281–300; b) S. B. Zimmerman, S. O. Trach, *J. Mol. Biol.* **1991**, *222*, 599–620.

[2] a) M. M. Dedmon, C. N. Patel, G. B. Young, G. J. Pielak, *Proc. Natl. Acad. Sci. USA* **2002**, *99*, 12681–12684; b) L. M. Luh, R. Hänsel, F. Löhr, D. K. Kirchner, K. Krauskopf, S. Pitzius, B. Schäfer, P. Tufar, I. Corbeski, P. Güntert, V. Dötsch, *J. Am. Chem. Soc.* **2013**, *135*, 13796–13803; c) A. Christiansen, P. Wittung-Stafshede, *Biophys. J.* **2013**, *105*, 1689–1699; d) C.

Echeverria, R. Kapral, *Phys. Chem. Chem. Phys.* **2012**, *14*, 6755 – 6763; e) B. Akabayov, S. R. Akabayov, S.-J. Lee, G. Wagner, C. C. Richardson, *Nat. Commun.* **2013**, *4*, 1615; f) N. F. Dupuis, E. D. Holmstrom, D. J. Nesbitt, *Proc. Natl. Acad. Sci. USA* **2014**, *111*, 8464 – 8469; g) R. Desai, D. Kilburn, H.-T. Lee, S. A. Woodson, *J. Biol. Chem.* **2014**, *289*, 2972 – 2977; h) D. T. Kulp, J. Herzfeld, *Biophys. Chem.* **1995**, *57*, 93 – 102; i) L. Breydo, K. D. Reddy, A. Piai, I. C. Felli, R. Pierattelli, V. N. Uversky, *Biochim. Biophys. Acta Proteins Proteomics* **2014**, *1844*, 346 – 357; j) M. D. Shtilerman, T. T. Ding, P. T. Lansbury, *Biochemistry* **2002**, *41*, 3855 – 3860; k) X.-D. Luo, F.-L. Kong, H.-B. Dang, J. Chen, Y. Liang, *Biochim. Biophys. Acta Proteins Proteomics* **2016**, *1864*, 1609 – 1619.

[3] M.. S. Cheung, A. G. Gasic, *Phys. Biol.* **2018**, *15*, 063001.

[4] P. B. Crowley, E. Show, T. Papkovskaia, *ChemBioChem* **2011**, *12*, 1043 – 1048.

[5] a) A. J. Guseman, S. L. Speer, G. M. Perez Goncalves, G. J. Pielak, *Biochemistry* **2018**, *57*, 1681 – 1684; b) A. E. Smith, L. Z. Zhou, A. H. Gorensek, M. Senske, G. J. Pielak, *Proc. Natl. Acad. Sci. USA* **2016**, *113*, 1725 – 1730; c) J. Danielsson, X. Mu, L. Lang, H. Wang, A. Binolfi, F.-X. Theillet, B. Bekei, D. T. Logan, P. Selenko, H. Wennerström, M. Oliveberg, *Proc. Natl. Acad. Sci. USA* **2015**, *112*, 12402 – 12407; d) S. Sukenik, M. Salam, Y. Wang, M. Gruebele, *J. Am. Chem. Soc.* **2018**, *140*, 10497 – 10503.

[6] a) L. Sapir, D. Harries, *J. Phys. Chem. Lett.* **2014**, *5*, 1061 – 1065; b) P.-h. Wang, I. Yu, M. Feig, Y. Sugita, *Chem. Phys. Lett.* **2017**, *671*, 63 – 70; c) P. Dey, A. Bhattacherjee, *Sci. Rep.* **2018**, *8*, 844.

[7] S. Qin, H.-X. Zhou, *Curr. Opin. Struct. Biol.* **2017**, *43*, 28 – 37.

[8] A. P. Minton, *Biopolymers* **1981**, *20*, 2093 – 2120.

[9] G. Rivas, A. P. Minton, *Biophys. Rev. Lett.* **2018**, *10*, 241 – 253.

[10] a) P. B. Crowley, K. Brett, J. Muldoon, *ChemBioChem* **2008**, *9*, 685 – 688; b) M. Senske, D. Constantinescu-Aruxandei, M. Havenith, C. Herrmann, H. Weingärtner, S. Ebbinghaus, *Phys. Chem. Chem. Phys.* **2016**, *18*, 29698 – 29708.

[11] a) V. Ittah, E. Kahana, D. Amir, E. Haas, *J. Mol. Recognit.* **2004**, *17*, 448 – 455; b) M. Candotti, M. Orozco, *PLoS Comput. Biol.* **2016**, *12*, e1005040; c) Y. Wang, H. He, S. Li, *Biochemistry (Moscow)* **2010**, *75*, 648 – 654.

[12] a) A. Schnuchel, R. Wiltscheck, M. Czisch, M. Herrier, G. Willemsky, P. Graumann, M. A. Marahiel, T. A. Holak, *Nature* **1993**, *364*, 169 – 171; b) H. Schindelin, M. A. Marahiel, U. Heinemann, *Nature* **1993**, *364*, 164 – 168; c) T. Schindler, M. Herrler, M. A. Marahiel, F. X. Schmid, *Nat. Struct. Biol.* **1995**, *2*, 663 – 673.

[13] M. Senske, L. Törk, B. Born, M. Havenith, C. Herrmann, S. Ebbinghaus, *J. Am. Chem. Soc.* **2014**, *136*, 9036 – 9041.

[14] K. Sasahara, P. McPhie, A. P. Minton, *J. Mol. Biol.* **2003**, *326*, 1227 – 1237.

[15] a) N. H. Andersen, J. W. Neidigh, S. M. Harris, G. M. Lee, Z. Liu, H. Tong, *J. Am. Chem. Soc.* **1997**, *119*, 8547 – 8561; b) T. Cierpicki, J. Otlewski, *J. Biomol. NMR* **2001**, *21*, 249 – 261; c) T. Cierpicki, I. Zhukov, R. A. Byrd, J. Otlewski, *J. Magn. Reson.* **2002**, *157*, 178 – 180; d) J. H. Tomlinson, M. P. Williamson, *J. Biomol. NMR* **2012**, *52*, 57 – 64.

[16] a) G. Gemmecker, W. Jahnke, H. Kessler, *J. Am. Chem. Soc.* **1993**, *115*, 11620 – 11621; b) S. Koide, W. Jahnke, P. E. Wright, *J. Biomol. NMR* **1995**, *6*, 306 – 312; c) S. Mori, C. Abeygunawardana, J. M. Berg, P. C. M. van Zijl, *J. Am. Chem. Soc.* **1997**, *119*, 6844 – 6852; d) H. Hofmann, U. Weininger, C. Löw, R. P. Golbik, J. Balbach, R. Ulbrich-Hofmann, *J. Am. Chem. Soc.* **2009**, *131*, 140 – 146.

[17] A. Schluck, G. Maurer, M.-R. Kula, *Biotechnol. Bioeng.* **1995**, *47*, 252 – 260.

Manuscript received: November 6, 2018

Accepted manuscript online: December 3, 2018

Version of record online: February 11, 2019

